General Disclaimer

One or more of the Following Statements may affect this Document

- This document has been reproduced from the best copy furnished by the organizational source. It is being released in the interest of making available as much information as possible.

- This document may contain data, which exceeds the sheet parameters. It was furnished in this condition by the organizational source and is the best copy available.

- This document may contain tone-on-tone or color graphs, charts and/or pictures, which have been reproduced in black and white.

- This document is paginated as submitted by the original source.

- Portions of this document are not fully legible due to the historical nature of some of the material. However, it is the best reproduction available from the original submission.

Electrochemical Investigation of Corrosion in the Space Shuttle Launch Environment

L.M. Calle

National Aeronautics and Space Administration (NASA)
Kennedy Space Center, Florida USA

Abstract

Corrosion studies began at NASA/Kennedy Space Center in 1966 during the Gemini/Apollo Programs with the evaluation of long-term protective coatings for the atmospheric protection of carbon steel. An outdoor exposure facility on the beach near the launch pad was established for this purpose at that time. The site has provided over 35 years of technical information on the evaluation of the long-term corrosion performance of many materials and coatings as well as on maintenance procedures. Results from these evaluations have helped NASA find new materials and processes that increase the safety and reliability of our flight hardware, launch structures, and ground support equipment. The launch environment at the Kennedy Space Center (KSC) is extremely corrosive due to the combination of ocean salt spray, heat, humidity, and sunlight. With the introduction of the Space Shuttle in 1981, the already highly corrosive conditions at the launch pad were rendered even more severe by the acidic exhaust from the solid rocker boosters. It has been estimated that 70 tons of hydrochloric acid (HCl) are produced during a launch.

The Corrosion Laboratory at NASA/KSC was established in 1985 to conduct electrochemical studies of corrosion on materials and coatings under conditions similar to those encountered at the launch pads. I will present highlights of some of these investigations.

Introduction

The Kennedy Space Center (KSC) is a major source of corrosion expertise. The launch environment at KSC is extremely corrosive due to the combination of ocean salt spray, heat, humidity, and sunlight. With the introduction of the Space Shuttle in 1981, the already highly corrosive conditions at the launch pad were rendered even more severe by the acidic exhaust from the solid rocket boosters.

Currently, KSC has to maintain about $2 billion worth of unique equipment and facilities, not including the orbiters, valued at about $8 billion. Among the items: two launch complexes, two crawler transporters, three mobile launch platforms, and specialized testing equipment.[1]

Corrosion studies began at KSC in 1966 during the Gemini/Apollo Programs with the evaluation of long-term protective coatings for the atmospheric protection of carbon steel. NASA's KSC Beach Corrosion Test Site (BCTS) was established at that time (Figure 1). In the years that followed, numerous studies at the site have identified materials, coatings, and maintenance procedures for launch hardware and equipment exposed to the highly corrosive

environment at the launch pad. Results from these evaluations have helped KSC find new materials and processes that increase the safety and reliability of our launch structures and ground support equipment.

Figure 1. KCS's Beach corrosion Test Site

The BCTS has been documented as having the highest corrosivity of any long-term exposure site in North America and one of the highest in the world.[2] Table 1 compares the corrosivity of the BCTS location with other test sites. Figure 2 shows the rapid decrease in corrosion rates as distance from the BCTS increases.

Table 1. Comparison of corrosion rates of carbon steel at various test locations

Location	Type Of Environment	µm/yr	Corrosion rate (a) mils/yr
Esquimalt, Vancouver Island, BC, Canada	Rural marine	13	0.5
Pittsburgh, PA	Industrial	30	1.2
Cleveland, OH	Industrial	38	1.5
Limon Bay, Panama, CZ	Tropical marine	61	2.4
East Chicago, IL	Industrial	84	3.3
Brazos River, TX	Industrial marine	94	3.7
Daytona Beach, FL	Marine	295	11.6
Pont Reyes, CA	Marine	500	19.7
Kure Beach, NC (80 ft. from ocean)	Marine	533	21
Galeta Point Beach, Panama CZ	Marine	686	27
Kennedy Space Center, FL (beach)	Marine	1070	42

(a) Two-year average

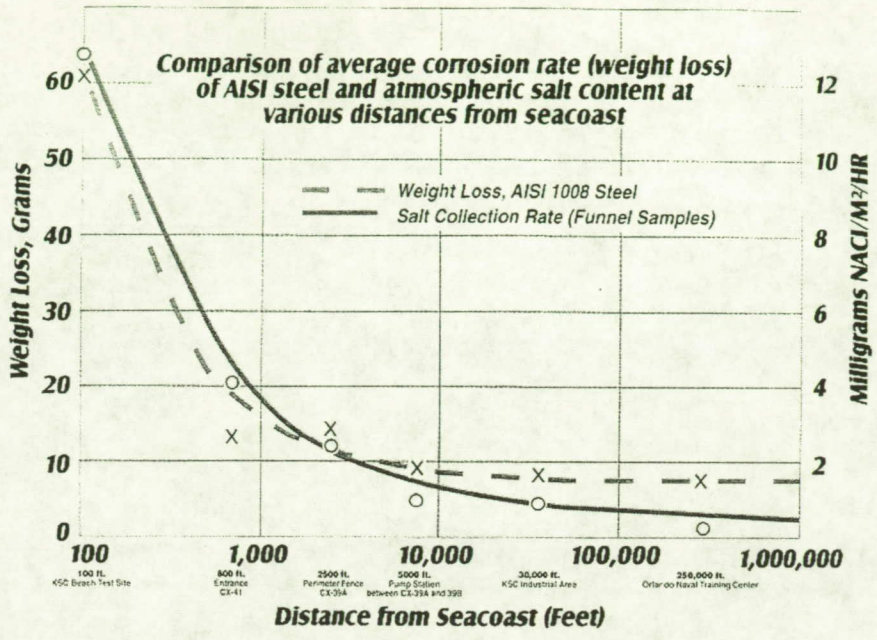

Figure 2. Changes of corrosion rate with distance from the ocean[3]

Over the years, many alloys have been evaluated for their corrosion performance under conditions similar to those found at the launch pads. These studies have included atmospheric exposure end evaluation with conventional electrochemical methods like open circuit potential (OCP) measurements, polarization techniques, and electrochemical impedance spectroscopy (EIS).

In 1987, a study was initiated to find a replacement alloy for the 304 stainless steel in the metal flex hoses used in various supply lines that service the Orbiter at the launch pad. These convoluted flexible hoses, which were originally made out of 304L stainless steel, had failed due to pitting. In the case of vacuum jacketed cryogenic lines, pinhole leaks, caused by failure of the flex hose, produced a loss of vacuum and subsequent loss of insulation. Nineteen alloys were investigated and evaluated using a variety of techniques that included exposure at the BCTS, electrochemical characterization, Salt Fog Chamber Exposure, and Ferric Chloride Immersion. As a result of that study, a nickel-chromium-molybdenum-tungsten substitute alloy was identified to replace the 304 stainless steel in use. Flex hoses made of this alloy are now performing without failure due to corrosion at the launch pad since 1988.[4]

A current investigation is underway to study the corrosion behavior of corrosion resistant alloys to replace the 304L stainless steel tubing at the Space Shuttle launch sites. The alloys include 317L, 316L, 254-SMO, AL-6XN, AL29-4C, and 304L as a control. 304L stainless

steel tubing is susceptible to pitting corrosion and Stress Corrosion Cracking (SCC)[5] Use of corrosion resistant tubing will greatly reduce the probability of future corrosion failures, improve safety, and reduce maintenance costs.

Materials and Methods

Table 2 lists the tubing alloys chosen for this investigation. Table 3 lists common name, UNS number, and chemical composition of each material. The specimens were flat sample coupons, 3.2 cm in diameter, from Metal Samples Co. The test specimens were polished to 600-grit, ultrasonically degreased in a detergent solution, and wiped with acetone before testing.

Table 2. Alloys included in this investigation

Alloy	Class
304L	Low carbon austenitic stainless steel
316L	Molybdenum-containing austenitic stainless steel
317L	Molybdenum-containing austenitic stainless steel
AL-6XN	Superaustenitic stainless steel
AL29-4C	Superferritic stainless steel
254-SMO	Austenitic stainless steel

A model 352 SoftCorr^{TM} III Corrosion Measurement System, manufactured by EG&G Princeton Applied Research, was used for all electrochemical measurements. The equipment includes software designed to measure and analyze corrosion data. The electrochemical flat cell included a saturated calomel reference electrode, SCE, a platinum-on-niobium counter electrode, the working electrode, and a bubbler/vent tube. The specimen holder in the cell is designed such that the exposed metal surface area is 1 cm^2.

Three different aerated electrolyte solutions were used: 3.55% NaCl, 3.55% NaCl–0.1N HCl and 3.55% NaCl–1.0N HCl. These solutions emulate less than, similar to, and more aggressive conditions respectively than those found at the launch pads at KSC.

Corrosion potential, linear, and cyclic polarization data were gathered for the alloys under the three different electrolyte conditions. Polarization resistance determinations were generally based on ASTM G 59.[6] Cyclic polarization data were gathered using ASTM G 61[7] as a guideline. Duplicate and triplicate tests had essentially the same outcome. The reported results are the averages of two or more runs.

A potential range of ±20 mV versus open circuit potential was used for the linear polarization measurements. The scan rate was 0.166 mV/sec. A linear graph of potential (E) versus current (I) was obtained and the polarization resistance (R_p) calculated.

Cyclic polarization measurements were started at –250mV relative to the corrosion potential (E_{corr}). The scan rate was 0.166mV/sec. The scans were reversed when the current

density reached 5mA/cm^2. The reverse potential scan continued until the potential returned to the starting potential of –250 mV relative to E_{corr}. A graph of E versus Log (I) was obtained. From this graph, the breakdown potential (E_{bd}), repassivation potential (E_{rp}), and the area of the hysteresis loop were obtained. Linear and cyclic polarization results were calculated using the SoftCorr III software.

Table 3. Chemical composition of stainless steels alloys

Alloy	304L	316L	317L	AL-6XN	AL29-4C	254-SMO
UNS Number	S30403	S31603	S31703	N08367	S44735	S31254
Fe	71.567	69.053	63.525	48.118	66.594	55.162
Ni	8.200	10.140	13.200	23.88	0.260	17.900
Cr	18.33	16.240	18.100	20.470	28.750	20.000
Mo	0.500	2.070	3.160	6.260	3.780	6.050
Mn	1.470	1.780	1.510	0.300	0.260	0.490
C	0.023	0.019	0.017	0.020	0.020	0.012
N	0.030	0.050	0.030	0.330	0.031	0.196
Si	0.380	0.280	0.460	0.40	0.280	0.350
P	0.030	0.027	0.027	0.021	0.023	0.019
S	0.0002	0.001	0.001	0.0003	0.002	0.001
Cu	0.460	0.340	0.150	0.200		0.680
Co		0.240				
Nb					0.290	
Ti					0.360	

Results and Discussion

Corrosion Potential

Corrosion potential gives an indication of how noble a metal is in a given environment. In general, a more positive corrosion potential means that the metal can be expected to be more resistant to corrosion in that particular electrolyte than one with a more negative corrosion potential. Thus, most metals can be ranked according to resistance to corrosion based on corrosion potential. However, ranking corrosion resistance based on corrosion potential is not very reliable. Therefore, other methods are used to determine actual or likely corrosion behavior. Stainless steels can exhibit active or noble potentials depending on whether they incur corrosion or are in a passive state. This depends on the environment and other factors.

The corrosion potential for each alloy was monitored from the initial time of immersion until a stable potential was observed. The alloys differed in the time it took for the potential to stabilize. For simplicity, Figure 3 shows only the open circuit potential for the SS alloys at times just prior to and during stabilization. Table 4 lists the average value of the stable open circuit potential. Contrary to what was expected based on the composition of the alloys, the highly alloyed SS 254-SMO, AL-6XN and AL29-4C did not exhibit a more noble stable potential when

compared to 316L and 317L in 3.55% NaCl (Figure 3a). This behavior did not correlate with the performance of the tubing samples exposed to the atmosphere at the corrosion test site. As it was expected, 304L was the most active alloy in this environment with a stable corrosion potential of –173 mV vs. SCE.

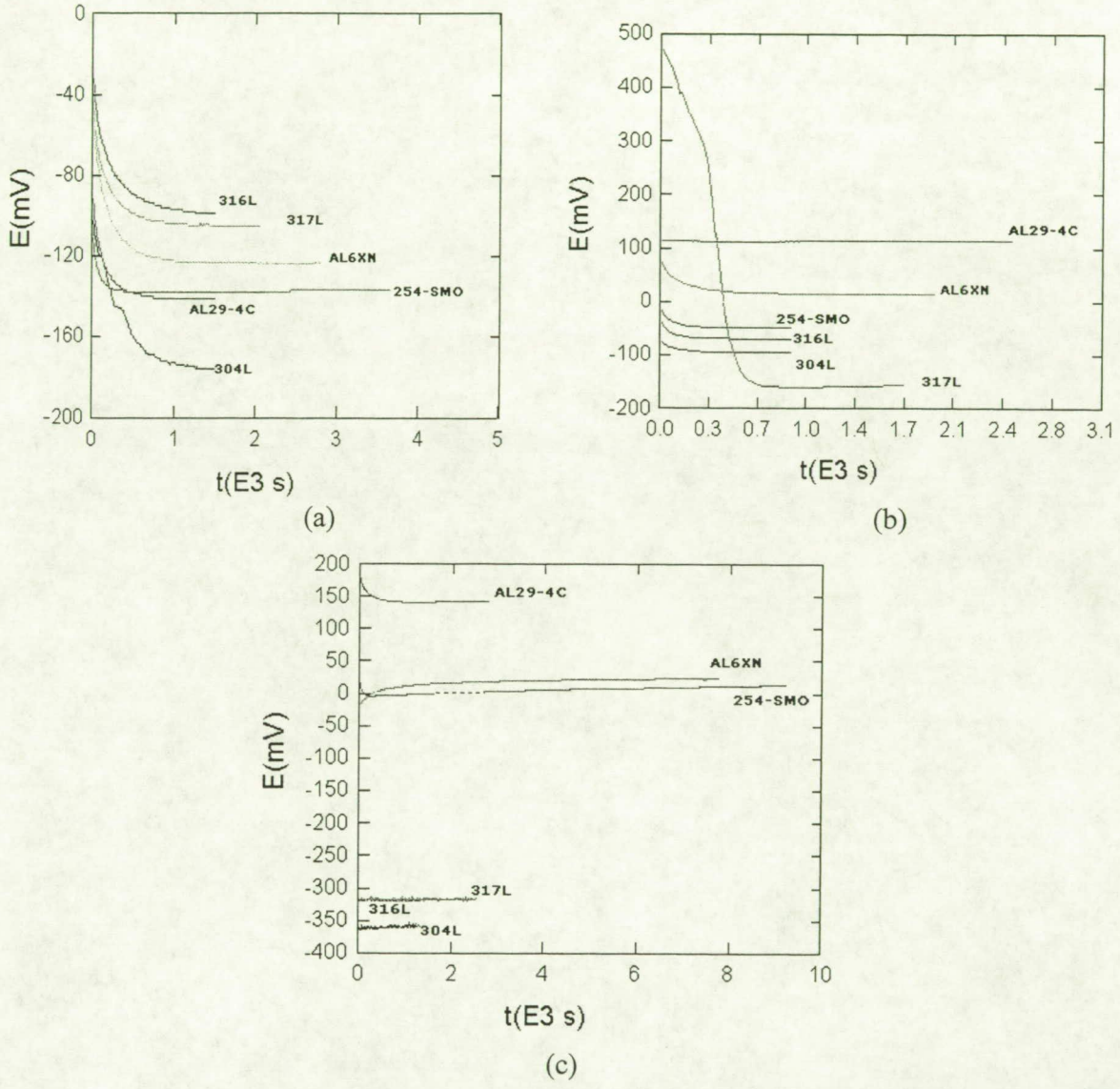

Figure 3. Corrosion potential of SS Alloys in (a) neutral 3.55% NaCl, (b) 3.55% NaCl-0.1N HCl, and (c) 3.55% NaCl-1.0N HCl.

Table 4. Corrosion Potentials of alloys

Alloy	E_{corr} (mV)		
	Neutral	**0.1N HCl**	**1.0N HCl**
304L	-155	-122	-349
316L	-102	-130	-320
317L	-111	-150	-318
AL-6XN	-125	12	28
AL29-4C	-132	110	137
254 SMO	-132	-48	12

In 3.55% NaCl-0.1N HCl, the three highly alloyed SS displayed a more noble potential than the 300 series SS as it was expected based on their composition. This behavior became more pronounced when the concentration of HCl in the 3.55% NaCl solution was increased to 1.0N. Figure 5c shows a clear distinction between the more noble behavior of the highly alloyed SS in the 3.55% NaCl-1.0N HCl and the more active behavior of the 300 series SS. The ennoblement of the higher alloyed SS as the concentration of HCl, in the 3.55% NaCl solution, increased was most pronounced for AL29-4C (269 mV increase in the corrosion potential) followed by AL-6XN (153 mV increase) and 254 SMO (144 mV increase). This behavior correlated very well with the actual corrosion performance of the alloys under atmospheric exposure. The transition toward a more active corrosion potential of the 300 series SS as the concentration of HCl in the electrolyte increased can be attributed to the fact that these alloys are easily attacked by HCl because the passive film is not easily attained. Chloride (Cl^-) ions are well known for their ability to attack SS by penetrating the protective layer at any discontinuity of the oxide film. The addition of HCl, a reducing acid, exacerbates the attack by interfering with the formation of the oxide film.[8]

Polarization Resistance

Figure 4 shows linear polarization plots for SS 316L in 3.55% NaCl with increasing HCl concentrations (neutral (a), 0.1N (b), and 1.0N (c)). It is evident from the figure that the slope of the line decreases as the acidity of the 3.55% NaCl solution increases. This behavior is indicative of the decrease in the polarization resistance. Table 5 summarizes the polarization resistance, R_p, values in neutral 3.55% NaCl, 3.55% NaCl-0.1N HCl, and in 3.55% NaCl-1.0N HCl for all the alloys. The R_p values show that increasing the HCl concentration in the 3.55% NaCl solution resulted in a significant decrease in the R_p values of the 300 series SS. The decrease in the R_p values, indicative of an increase in the corrosion rate, in the presence of increasing concentrations of HCl, can be attributed to the fact that the protective layer of the 300 series SS becomes unstable. This is illustrated by the drastic decrease in R_p from 1.36 Mohms.cm^2 in neutral 3.55% NaCl to 159 ohms.cm^2 in 3.55%NaCl-1.0N HCl for 316L (Figure 4 and Table 5).

R_p values for AL-6XN, AL29-4C, and 254-SMO in neutral 3.55% NaCl were approximately of the same order of magnitude as those for the 300 series SS. However, the R_p values for these alloys remained high as the concentration of HCl in the 3.55% NaCl solution increased. AL-6XN

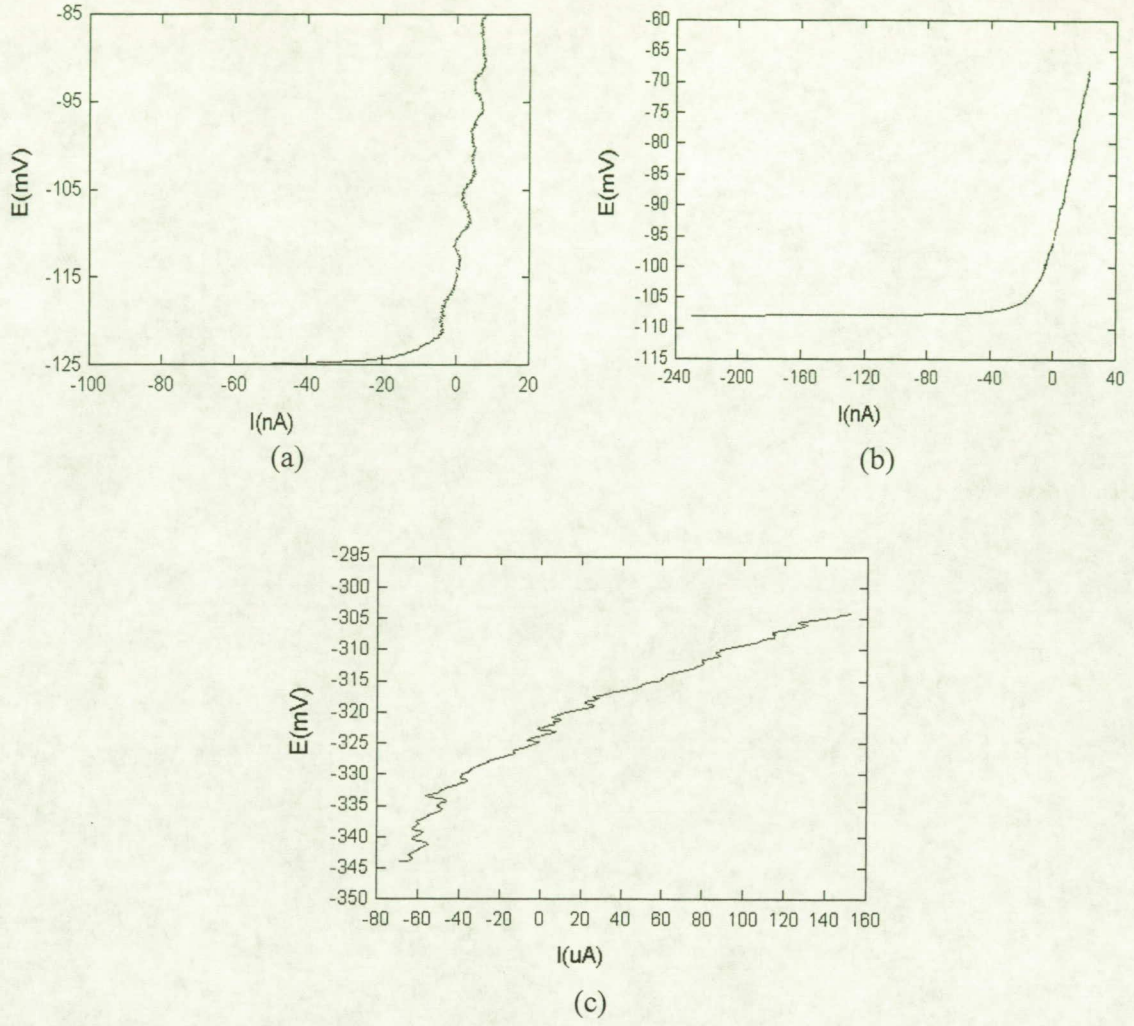

Figure 4. Linear polarization curves for 316L in (a) neutral 3.55% NaCl, (b) 3.55% NaCl-0.1N HCl, and (c) 3.55% NaCl-1.0N HCl

Table 5. Polarization resistance of SS alloys in 3.55% nacl in various concentrations of HCl

Alloy	R_p (ohms.cm^2)		
	Neutral	**0.1N HCl**	**1.0N HCl**
304L	6.37×10^5	7.05×10^5	2.00×10^2
316L	1.36×10^6	4.80×10^5	1.59×10^2
317L	1.49×10^6	2.99×10^5	1.93×10^2
AL-6XN	1.40×10^6	1.18×10^6	0.615×10^6
AL29-4C	0.882×10^6	1.09×10^6	1.09×10^6
254 SMO	1.08×10^6	1.01×10^6	0.782×10^6

and 254-SMO showed a slight decrease in R_p as the concentration of HCl increased while AL29-4C exhibited no change in Rp after the initial slight increase. The lower corrosion rates of AL-6XN, AL29-4C, and 254-SMO SS can be attributed to the presence of greater amounts of chromium, nickel and molybdenum that result in a more stable protective layer on the surface of the alloy. The low corrosion rate of AL29-4C, which remained fairly unchanged with the increased concentration of HCl, can be attributed to its high (28.750%) chromium content.

Cyclic Polarization

Cyclic Polarization measurements were performed in order to determine the tendency of the alloys to undergo localized (pitting or crevice) corrosion when placed in the electrolyte solutions. The resulting plot of the potential-current function is strongly indicative of the tendency of the material to undergo localized attack. In effect, the function traces a hysteresis loop, with the area of the loop indicating the amount of localized corrosion of the material. From the area value, it is possible to analyze the performance of the alloys. Hysteresis loop area values should be very small for alloys that are highly resistant to localized corrosion. In this case, the reverse scan traces almost exactly over the forward scan.[9-10]

Two important potentials, also used to characterize the hysteresis loop, are the critical breakdown potential, E_{bd}, defined as the potential forward scan "knee" potential. Pitting is characterized by a rapid increase in current with a very small change in potential. Above this potential, pits initiate and propagate. The repassivation potential, E_{rp}, is defined as the point where the reverse scan intersects the forward scan. At this potential, localized attack stops and the current decreases significantly past the passive current density. The more positive the value of E_{bd}, the more resistant the alloy is to initiation of localized corrosion. Also, the more positive the value of E_{rp}, the more resistant the alloy to corrosion is.[6] Values of E_{bd} and E_{rp} for the SS alloys in the three different electrolytes are shown in Table 5.

Cyclic polarization scans for three of the alloys included in this investigation are shown in Figures 5-7. Hysteresis loop area values are given in Table 6. Figure 5 shows a cyclic polarization scan for SS AL29-4C in 3.55% NaCl-1.0N HCl. In this case, the reverse scan traced almost exactly over the forward scan resulting in no hysteresis. This is characteristic of an alloy that is highly resistant to localized corrosion. Figure 6 shows the overlay of the cyclic polarization scans for SS 316L and SS 254-SMO in 3.55% NaCl-1.0N HCl.

The hysteresis loop area values for these two alloys are very similar under these conditions (5.58 and 5.98 coulombs respectively) indicating a high resistant to localized corrosion. However, because of the significance of E_{bd} and E_{rp}, it is important to take also into account the position of the scan in the E vs. Log (I) diagram when analyzing cyclic polarization data. While the area of the hysteresis loop is very similar, Figure 6, the position of the scans in the plot is very different. The values of E_{bd} and E_{rp} for 316L are –42 mV and –37 mV respectively, while the values for 254-SMO are 877 mV and 890 mV. These results indicate that 254-SMO is a superior alloy in its corrosion resistance to localized corrosion when compared to 316L under the same conditions. Similar results were obtained for AL-6XN and AL29-4C.

Table 5. Critical breakdown and repassivation potentials for SS alloys in 3.55% NaCl in various concentrations of HCl

Alloy	Neutral E_{bd} (mV) E_{rp} (mV)		0.1N HCl E_{bd} (mV) E_{rp} (mV)		1.0N HCl E_{bd} (mV) E_{rp} (mV)	
304L	366	-136	167	-153	-60	-58
316L	380	-143	135	-164	-42	-37
317L	622	-131	432	-91	-90	-89
AL-6XN	922	906	816	835	902	904
AL29-4C	964	964	818	N/A	878	N/A
254 SMO	952	939	825	831	877	890

Table 6. Area of hysteresis loop for SS alloys in 3.55% NaCl with various concentrations of HCl

	Area of Hysteresis Loop (Coulombs)		
Alloy	**Neutral**	**0.1N HCl**	**1.0N HCl**
304L	22.96	11.36	10.42
316L	15.99	12.35	5.58
317L	33.12	23.53	12.58
AL-6XN	5.07	3.23	1.69
AL29-4C	5.23	Negative	No
254 SMO	5.11	4.85	5.98

SS AL29-4C is an alloy very resistive to localized corrosion as indicated by the very small hysteresis loop area in the cyclic polarization scan obtained in neutral 3.55% NaCl. The increase in the acid concentration of the 3.55% NaCl solution to 0.1N resulted in a negative hysteresis. A further increase to 1.0N in the concentration of the acid resulted in no hysteresis, Figure 5. SS AL-6XN and 254 SMO exhibited small hysteresis loop areas in the three electrolytes indicative of their resistance to localized corrosion in neutral and acidic 3.55% NaCl.

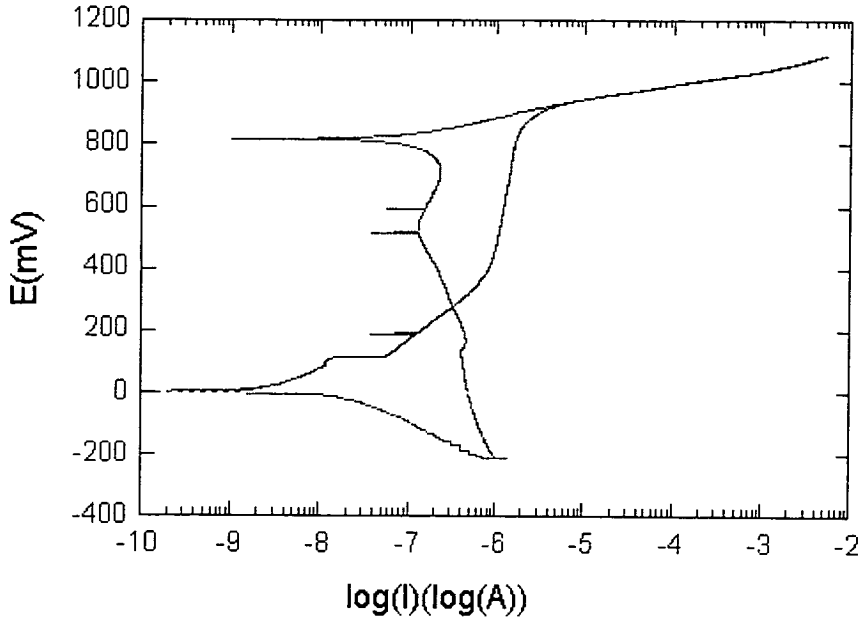

Figure 7. Cyclic polarization for AL29-4C in 3.55% NaCl-1.0N HCl

Figure 7 shows the effect of increasing HCl concentration on the cyclic polarization scans of SS 304L. The scan in neutral 3.55% NaCl solution displays a higher corrosion potential as well as lower current density. When the HCl concentration was increased to 0.1N, the corrosion potential became more negative and the current density increased. The metal still portrays passive behavior where the voltage increases with small changes in current density. However, increasing the acid concentration to1.0N HCl affects the alloy more drastically. Past the corrosion potential, the material experiences anodic dissolution and then repassivates over a small voltage range and rapidly experiences breakdown of the passive film at E_{bd}. Similar behavior was observed for the other 300 series SS. For these alloys, a decrease in the hysteresis loop area cannot be interpreted as an indication of increased resistance to localized corrosion.

A decrease in the difference between E_{corr} and E_{bd} has been associated with increased susceptibility to localized corrosion.[12] Table 7 shows the values for the difference between E_{corr} and E_{bd} for the SS alloys in the three different electrolytes. The values for the 300 series SS are lower than those for the higher alloyed materials and their decrease as the concentration of acid in the electrolyte increases is greater than for the higher alloyed materials. These results are in agreement with results from visual observations of the samples as well as with the atmospheric exposure data on the susceptibility to localized corrosion of these alloys.

Visual observation of the samples at the conclusion of the cyclic polarization measurements revealed that the 300 series SS samples experienced crevice corrosion in all three electrolytes. 254-SMO, AL-6XN and AL29-4C experienced some crevice corrosion but only under neutral conditions. This can be attributed to the fact that the interface between the metal coupon and the cell gasket creates a site favorable to crevice corrosion. The area of the loop from the cyclic

polarization scans accounts for both pitting and crevice corrosion whenever they are present. Breakdown or pitting potential as well as repassivation potential also correspond to crevice formation. The potential for initiation of crevice corrosion is more active than E_{pit} for the same alloy, because of the favorable geometric conditions for deaeretion and chloride concentration.[13]

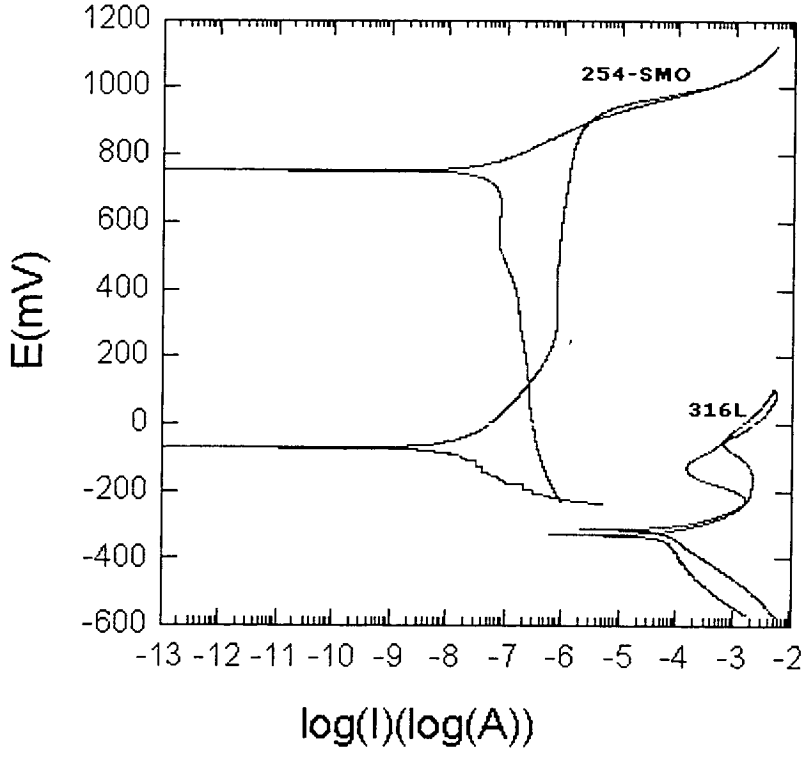

Figure 8. Cyclic polarization for 316L and 254-SMO in 1.0N-HCl 3.55% NaCl

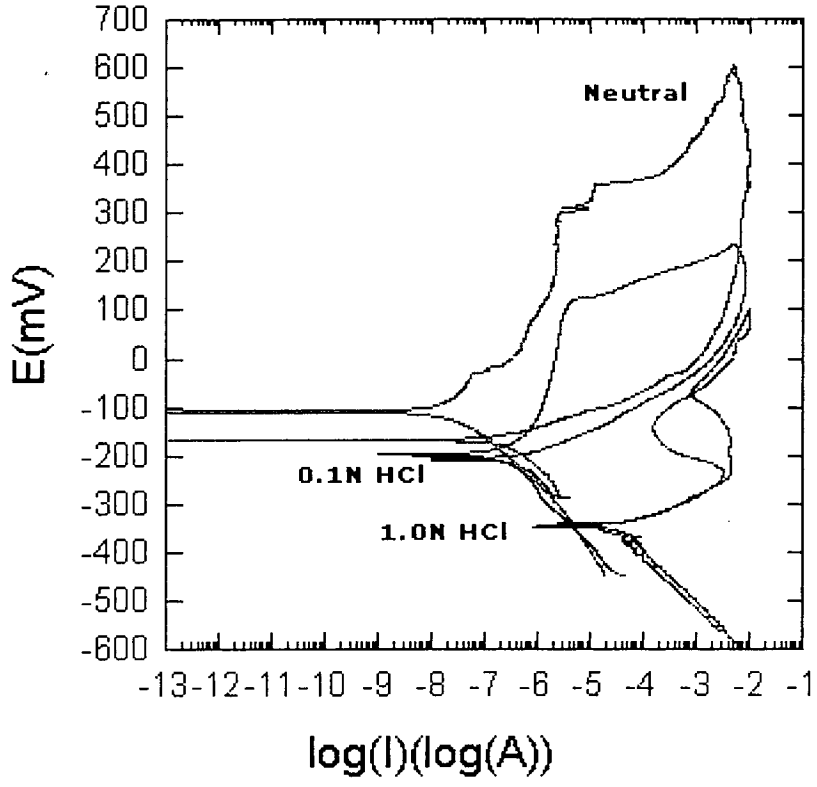

Figure 9. Cyclic polarization scans for 304L in neutral, 0.1N and 1.0N HCl-3.55% NaCl solutions

Table 7 Difference between E_{corr} and E_{bd} for SS alloys in 3.55% NaCl with various concentrations of hcl

	E_{bd}-E_{corr} (mV)		
Alloy	**Neutral**	**0.1N HCl**	**1.0N HCl**
304L	514	401	287
316L	510	424	271
317L	810	730	221
AL-6XN	1081	895	950
AL29-4C	1129	757	746
254 SMO	1106	978	944

Pitting Resistance Equivalent Number

It is well established that the pitting corrosion resistance of stainless steels depends mainly upon their chromium, molybdenum, and nitrogen contents. This resistance is evaluated empirically through the pitting resistance equivalent number (PREN) defined as:

$$PREN = (\%Cr) + (3.0) \times (\%Mo) + (15) \times (\%N)$$

where the percentage corresponds to the weight percentage of the element in the alloy.[14-16] PREN numbers for the alloys investigated are shown in Table 8. These values are in good agreement with the experimental results.

Table 8. PREN numbers for stainless steel alloys

Alloy	304L	316L	317L	AL-6XN	AL29-4C	254 SMO
PREN	19	26	31	46	40	43

Atmospheric Exposure

The most important criteria of any laboratory test for localized corrosion is that it must rate alloys consistently with service performance in environments that cause localized corrosion. In this study, the laboratory results were compared to the two-year atmospheric exposure data. Detailed results of the atmospheric exposure have been previously reported elsewhere.[17] Photographs of the tubes after one year of atmospheric exposure with no acid rinse are shown in Figure 8. Photographs of the tubes after two years of atmospheric exposure with biweekly acid rinse are shown in Figure 9. A photograph of SS 304L is not shown because the tube failed prior to the two-year evaluation and was removed from the test rack. A summary of the visual evaluation of the tubing test articles after two years of atmospheric exposure is shown in Table 9.

Table 9. Visual observations of tube specimens after two years of atmospheric exposure

Visual Observations after Two Years of Atmospheric Exposure		
Alloy	**Natural**	**With Acid-Alumina Slurry Rinse**
304L	Tubes in poor condition with pits and brown spots all over	Tubes failed due to pitting. Pits went through the thickness of the tube
316L	Tubes in poor condition with pits and brown stains. Better than 304L	2 out 3 tubes failed. Remaining tube in bad condition with brown spots and pits all over
317L	Brown spots and pits on the tube. Better than 316L	1 out 3 tubes failed. Pits and brown spots all over the tube. Better condition than 316L
AL-6XN	Light browning of the tube.	Tubes look in good condition with slight discoloration
AL29-4C	Slight discoloration of the tubes. Over all in good condition.	Tubes in good condition
254-SMO	Tube is in good condition. Some spots along the seam weld	Tubes look very good except for pits on the seam weld

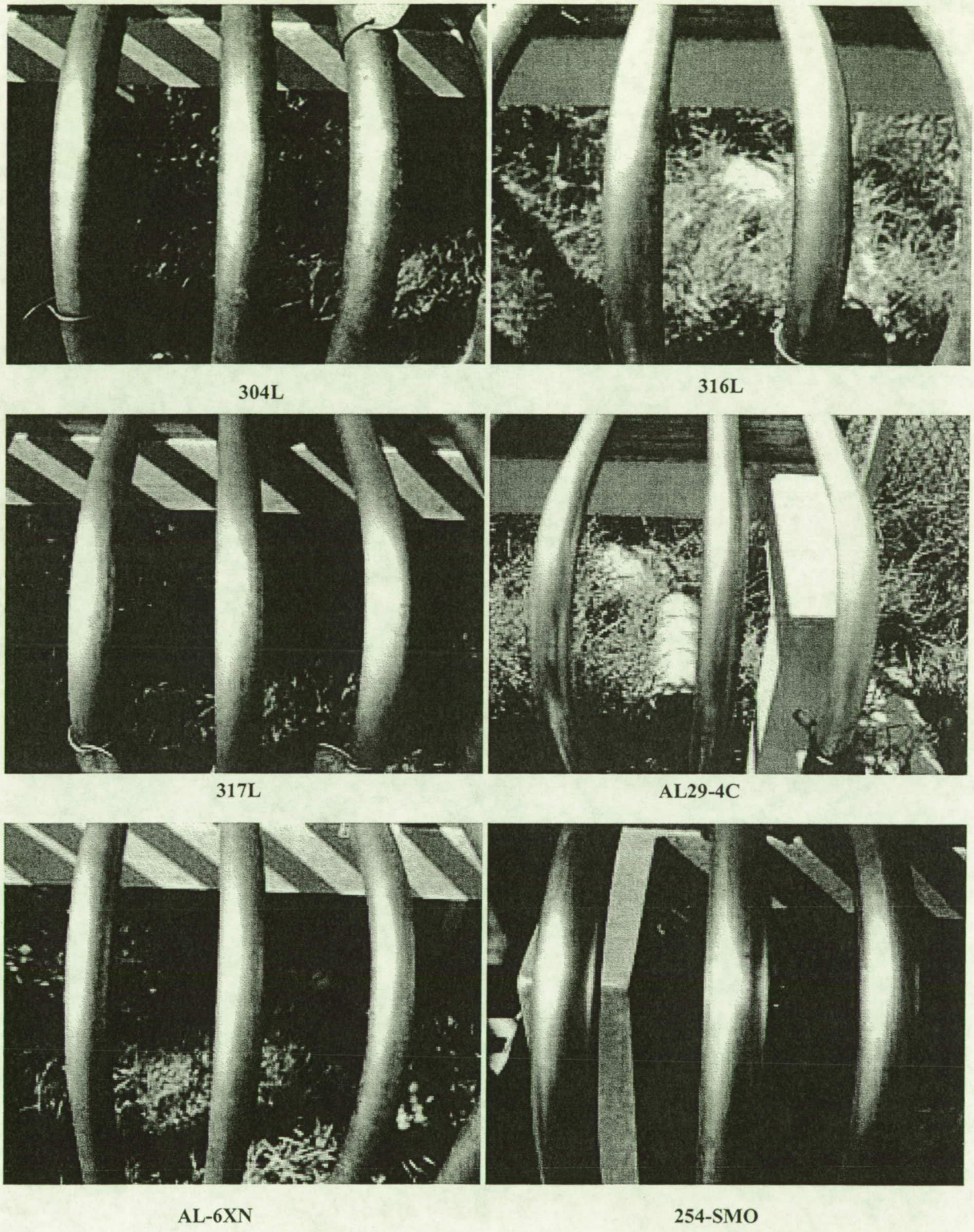

FIGURE 10. Tubing after one year of natural seacoast atmospheric exposure (no acid rinse).

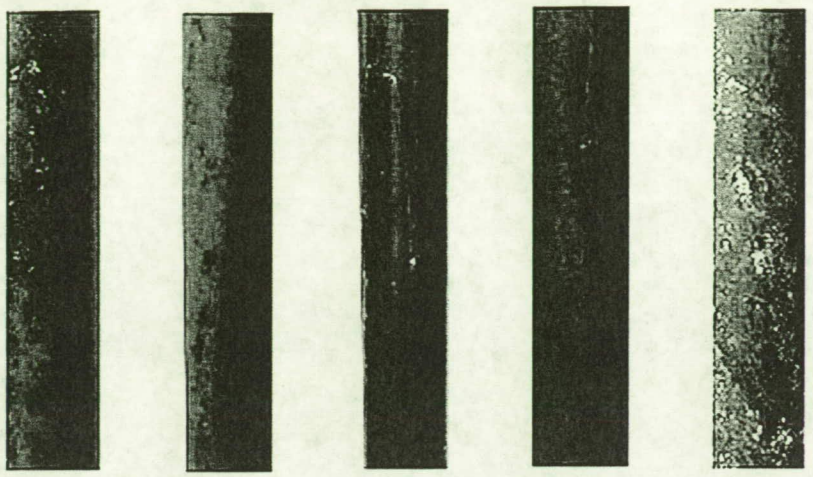

Figure 11. Photographs of tubing sections after two years of seacoast atmospheric exposure with acid rinse every two weeks.

Conclusions

Electrochemical measurements of the six alloys indicated that the higher alloyed SS 254 SMO, AL29-4C, and AL-6XN exhibited a significantly higher resistance to localized corrosion than the 300 series SS.

The stable corrosion potential values obtained in neutral 3.55% NaCl did not correlate with the performance of the alloys under natural seacoast atmospheric exposure.

A correlation was found between the stable corrosion potential values obtained in acidic 3.55% NaCl and the corrosion performance of the alloys under atmospheric exposure with and without acid rinse.

There was a correlation between the corrosion performance of the alloys during the two-year atmospheric exposure and the corrosion rates based on polarization resistance values.
The area of the hysteresis loop cannot be used as the sole criterion to predict susceptibility to localized corrosion.

There was a correlation between the atmospheric exposure data and the susceptibility to localized corrosion that was predicted based on the difference between E_{bd} and E_{corr}. These predictions were in agreement with the expectations based on the PREN calculated for the alloys.

References

1. Florida Today, January 15, 2002.

2. S. Coburn, Atmospheric Corrosion, in Metals Handbook, 9th ed, Vol. 1, Properties and Selection, Carbon Steels, American Society for Metals, Metals Park, Ohio, 1978, p.720
3. J.D. Morrison, Report on the Relative Corrosivity of Atmospheres at Various Distances from the Seacoast, NASA-Kennedy Space Center, Report MTB 099-74.

4. C. Ontiveros and L. G. MacDowell, Corrosion 90, Paper No. 94, NACE, 1990.

5. S.J. McDanels, Failure Analysis of Launch Pad Tubing, Microstructural Science, **25**, p. 125-129 (1998).

6. ASTM G 59 – 97 (Reapproved 2003), "Standard Test Method for Conducting Potentiodynamic Polarization Resistance Measurements" (West Conshohocken, PA: ASTM International, 2003).

7. ASTM G 61 – 86 (Reapproved 2003), "Standard Test Method for Conducting Cyclic Potentiodynamic Measurements for Localized Corrosion Susceptibility of Iron-, Nickel-, or Cobalt-Based Alloys" (West Conshohocken, PA: ASTM International, 2003).

8. N.G. Thompson and J.H. Pager, DC electrochemical Test Methods, p. 57, (Houston, TX: NACE International, 1986)

9. W.S. Tait, Corrosion, 34 (6) (1978): pp.214-217.

10. W.S. Tait, corrosion, 35 (7) (1979): pp. 296-300.

11. Z. Szklarska-Smialowska, M. Janik-Czacho, Corros. Sci. 11 12(1971): p. 901.

12. J. Beddoes and J. Gordon Parr, Introduction to Stainless Steels (ASM International, Materials Park, OH), 1999, p. 83.

13. D.A. Jones, Principles and Prevention of Corrosion (Prentice Hall, Upper Saddle River, NJ), Second Edition, 1996, p. 223,

14. M.J. Matthews, Metall. Mater. Technol. 5 (1982): p. 205.

15. C.A. Clark, P. Gentil, P. Guha, "Development of Improved Alloy Duplex Steel, ed. J. Van Liere (The Hague, The Netherlands: Netherlands instituut Voor Lastechniek, 1986).

16. A.J. Sedriks, Corrosion, Vol. 42, 7 (1986): p. 376.

17. R.G. Barile, L.G. MacDowell, J. Curran, L.M. Calle, and T. Hodge, "Corrosion of Stainless Steel tubing in a Spacecraft Launch Environment," Paper No. 02152, Corrosion/2002, 57th Annual Conference & Exposition, April 7-11, 2002, Denver, Colorado.